

Dichotomy in host environments and signs of recycled active galactic nuclei

Georgina V. Coldwell,^{1,2*} Diego G. Lambas,¹ Ilona K. Söchting³
and Sebastián Gurovich¹

¹*IATE, Observatorio Astronómico, Universidad Nacional de Córdoba, Laprida 854, 5000 Córdoba, Argentina*

²*Departamento de Física, Universidad de La Serena, Benavente 980, La Serena, Chile*

³*University of Oxford, Astrophysics, Denys Wilkinson Building, Keble Road, Oxford OX1 3RH*

Accepted 2009 June 22. Received 2009 June 22; in original form 2009 May 4

ABSTRACT

We analyse the relation between active galactic nuclei (AGN) host properties and large-scale environment for a representative red and blue AGN host galaxy sample selected from the Data Release 4 Sloan Digital Sky Survey. A comparison is made with two carefully constructed control samples of non-active galaxies, covering the same redshift range and colour baseline. The cross-correlation functions show that the density distribution of neighbours is almost identical for blue galaxies, either active or non-active. Although active red galaxies inhabit environments less dense compared to non-active red galaxies, both reside in environments considerably denser than those of blue hosts. Moreover, the radial density profile of AGN relative to galaxy group centres is less concentrated than galaxies. This is particularly evident when comparing red AGN and non-active galaxies.

The properties of the neighbouring galaxies of blue and red AGN and non active galaxies reflect this effect. While the neighbourhood of the blue samples is indistinguishable, the red AGN environs show an excess of blue-star-forming galaxies with respect to their non-active counterpart. On the other hand, the active and non-active blue systems have similar environments but markedly different morphological distributions, showing an excess of blue early-type AGN, which are argued to be late-stage mergers. This comparison reveals that the observable differences between active red and blue host galaxy properties including star formation history and AGN activity depends on the environment within which the galaxies form and evolve.

Key words: galaxies: active – galaxies: general – galaxies: statistics.

1 INTRODUCTION

The standard model of the active galactic nuclei (AGN) phenomenon includes the accretion of cold gas by massive black holes that lie at the centres of galaxies (Lynden-Bell 1969). Although there is considerable evidence to suggest that most massive galaxies harbour a central black hole (Tremaine et al. 2002; Marconi & Hunt 2003), not all massive galaxies in fact are active. The search for the underlying reason on the observed occurrence or absence of AGN in massive galaxy hosts has been intense, and although some progress has been made largely this question remains unanswered. Many of the details of the gas cooling and transportation processes that trigger and produce AGN activity remain open to debate, yet

several processes that initialize and facilitate the gas transport have been proposed.

Toomre & Toomre (1972) suggest that collision-driven disruption and gas dissipation may feed the nuclear activity of galaxies. It is likely that tidal torques generated during galaxy interactions also play some role in providing gas inflows that end up feeding central black holes (Sanders, Soifer & Scoville 1988) that power AGN. Nevertheless, recent studies (Coldwell & Lambas 2006; Li et al. 2006; Alonso et al. 2007) have found no statistical evidence that major galaxy interactions are an efficient mechanism for the triggering of nuclear activity. However, the effect that minor mergers (Roos 1981, 1985; Gaskell 1985; Hernquist & Mihos 1995) or galaxy harassment (Lake, Katz & Moore 1998) processes have on nuclear activity remains yet to be quantified. Some other triggering mechanisms have been suggested, for example, internal instabilities in the discs of barred galaxies that cause gas transfer (Shlosman, Begelman & Frank 1990) as well as other gas dynamical processes

*E-mail: georgina@mail.oac.uncor.edu

implied by the presence of multiple supermassive black holes found in the centres of some active host galaxies (Begelman, Blandford & Rees 1980). One must also consider that it is plausible that at any given time or for any given AGN type more than one mechanism plays a role. The relative contributions of these processes probably evolve with redshift.

The environments of galaxies play a significant role in their evolution and so understanding the relation of nuclear activity with host galaxy environment provides an alternative angle to this problem. So, bringing all these possibilities together the question that has yet to be answered is if nuclear activity is a temporary stage in the evolution common to all galaxies of a certain type or if it is induced by events outside the host galaxy (nature versus nurture). In the nature case, the environment of AGN hosts would be a simple reflection of the environment typical to non-active galaxies of similar type. Therefore, the environment of AGN host galaxies adds a much needed constraint in understanding the AGN phenomenology.

Considerable effort has gone into such an undertaking and some progress has been made. Li et al. (2006) compare the clustering of galaxies centred about narrow-line galaxies (type II AGN) to a matched non-active centred host sample environ. They find no significant difference in the clustering amplitude at a scale larger than $1 h^{-1}$ Mpc and only a weak signal of higher galaxy density in the AGN environs at scales smaller than $1 h^{-1}$ Mpc. Sorrentino, Radovich & Rifatto (2006) study the density of AGN environs, star-forming galaxies and normal galaxies and find no evidence of a relation between large-scale environment and AGN activity. Several other studies also indicate that AGN and quasars reside in environments of similar galaxy density as those of non-AGN galaxies (Smith, Boyle & Maddox 1995; Coldwell & Lambas 2006). Nevertheless, the physical properties of the neighbouring galaxies appear to be significantly different.

Interesting parallels are observed for low-redshift quasars. Even though the distribution of quasars follow the same general large-scale structure traced by galaxy clusters, they are less concentrated around galaxy cluster centres but instead, more likely to be found in the periphery of clusters and between possibly merging galaxy clusters (Söchting, Clowes & Campusano 2002, 2004). It is precisely in these environments that discs are more prevalent because dynamical effects that tend to remove baryons and destroy disc formation (e.g. ram pressure stripping, tidal forces, galaxy harassment) that are more pronounced in denser environments are less significant. Hence, galaxies in both quasar and AGN environs are particularly blue, discy and star forming compared to those in the vicinity of typical galaxies up to scales of $\sim 1 h^{-1}$ Mpc (Coldwell & Lambas 2003, 2006).

Could overdensities observed strictly locally around quasars (Serber et al. 2006) and AGN (Koulouridis et al. 2006) within $\sim 0.1 h^{-1}$ Mpc cause AGN activity through gas dynamical galaxy interactions? Interestingly, evidence to the affirmative have been presented by the above authors, who find that at larger scales ($\sim 1 h^{-1}$ Mpc) active objects inhabit regions with densities similar to that found for L^* galaxies, consistent with the results of Coldwell & Lambas (2006).

Biviano et al. (1997) suggest that the lower AGN fraction in galaxy clusters originally proposed by Dressler, Thompson & Shectman (1985) is due to differences in the morphological mixture of galaxies in cluster and field environments. Miller et al. (2003) on the other hand find little evidence of environmental dependence on AGN fraction by analysing Sloan Digital Sky Survey (SDSS) galaxies across a wide range of environments. In spite of this, Kauffmann et al. (2004) also analyse SDSS galax-

ies yet they find that AGN underpopulate regions of high galaxy density.

These seemingly contradictory findings indicate that the study of AGN environs is highly sensitive on implicit sample selection effects made in such an analysis. This paper attempts to resolve some of these issues, and seeks to answer the question if AGN host galaxies inhabit the same environs as their non-active counterparts with similar properties. In contrast with existing studies, however, to minimize implicit selection biases, we choose two AGN samples each selected from the two extremes of the AGN colour distribution that we match with non-active comparison samples that have the same colour distribution. Our method will increase the sensitivity of any environmental signal that may otherwise be diluted by noise induced by the averaging across a large baseline of galaxy type, a problem which we consider implicit in some of the aforementioned studies.

The layout of the paper is as follows. Section 2 describes the data and sample selection criteria. Section 3 contains the large-scale clustering analysis for our active and non-active galaxy environments. In Section 4, we analyse the mean density profiles around galaxy groups. An analysis of the morphology of AGN hosts is described in Section 5. In Section 6, we determine and compare properties of galaxies in neighbourhoods of both non-active and AGN hosts. We summarize the main conclusions of our study in Section 7.

The cosmological parameters adopted throughout this paper are: $\Omega = 0.3$, $\Omega_\lambda = 0.7$ and $H_0 = 100 \text{ km s}^{-1} \text{ Mpc}^{-1}$.

2 DATA

The SDSS (York et al. 2000) has mapped one-quarter of the entire sky in five optical bands and performed a deep redshift survey of galaxies, quasars and stars. The fourth Data Release, DR4, from SDSS provides a data base of some $\sim 500\,000$ galaxies with measured spectra. The five filters u , g , r , i and z cover the entire wavelength range of the CCD response function (Fukugita et al. 1996). The main galaxy sample is essentially a magnitude-limited spectroscopic sample [with a Petrosian (1976) magnitude] $r_{\text{lim}} < 17.77$, with most galaxies spanning a redshift range $0 < z < 0.25$ with a median redshift of 0.1 (Strauss et al. 2002).

Several important properties have been derived for various subsamples of SDSS galaxies: gas-phase metallicities; stellar masses; indicators of recent major starbursts; current total and specific star formation rates (SFRs); emission-line fluxes; etc. (Brinchmann et al. 2004; Tremonti et al. 2004) by spectroscopic targeting of the main galaxies as well as candidate regional members. A comprehensive study of SDSS type II AGN including classification scheme is undertaken in Kauffmann et al. (2003a) based on the standard emission-line ratio diagnostic diagrams.

2.1 Sample selection

AGN are often separated into two categories: type 1 AGN, where the black hole and the associated stellar continuum and emission-line regions (both broad and narrow) are viewed and type 2 AGN for which the broad emission-line region cannot be viewed because of relative orientation of an obscuring medium. In this paper, we investigate the properties of AGN hosts by comparing them to matched non-active galaxies. We present evidence of the nature of the AGN trigger/fuelling mechanism by focusing on environment. Since the observed properties of the host galaxies of type 1 AGN are often contaminated by the contribution of the central nucleus, only type 2

AGN are included in this investigation, although we expect our results to also apply to type 1 AGN environments because essentially they are the same phenomenon. The Baldwin, Phillips & Terlevich (1981) line-ratio diagram allows for the separation of type 2 AGN from normal star-forming galaxies by considering the intensity ratios of two pairs of relatively strong emission lines. The sample of type 2 AGN of Kauffmann et al. (2003a) was selected taking into account the relation between spectral lines, $[\text{O III}]\lambda 5007$, $\text{H}\beta$, $[\text{N II}]\lambda 6583$ and $\text{H}\alpha$ luminosities where an AGN is defined by

$$\log_{10}([\text{O III}]/\text{H}\beta) > 0.61 / [\log_{10}([\text{N II}/\text{H}\alpha]) - 0.05] + 1.3. \quad (1)$$

We use the type 2 AGN sample of Kauffmann et al. (2003a) as well as a control sample from the main spectroscopic SDSS galaxy sample.

The colours of galaxies can be used to discriminate the stellar populations and their evolution. In galaxy clusters, the larger fraction of red galaxies indicate an old stellar population with galaxies typically having a lower SFR, while galaxies in poor groups and the field are bluer and have higher SFR. Thus, from the type 2 AGN sample two subsamples were selected at the extremes of the colour distribution: a red sample targeting potential cluster AGN and a blue sample chosen to represent field AGN.

We divide the AGN sample according to $M_g - M_r$ colours using K and extinction-corrected absolute magnitudes (Blanton et al. 2003). Here, the red AGN are $M_g - M_r > 1$ and the blue AGN are $M_g - M_r < 0.6$. With these colour cuts, we are considering ap-

proximately only 5 per cent of both extremes of the galaxy colour distribution, within $0.06 < z < 0.11$. Each represents two very distinct populations of AGN host galaxies. The AGN samples are also restricted to have identical redshift distributions.

We compare the results obtained for the active host galaxy environment with two carefully selected control samples of non-active galaxy environments. Each of the galaxy control samples is selected with properties to match the AGN samples in redshift, luminosity, colour, stellar mass and mean stellar age, measured by the 4000 Å break strength distributions. These restrictions ensure that any difference in environmental properties can only be attributed to nuclear activity. We note that the stellar mass from SDSS AGN and galaxies have been previously determined by Kauffmann et al. (2003b) using a method that relies on spectral indicators of the stellar age and the fraction of stars formed in recent bursts. The break index $D_n(4000)$ (Kauffmann & Haehnelt 2002) is defined as the ratio of the average flux density in the narrow continuum bands (3850–3950 and 4000–4100 Å) and is suitably correlated to the mean age of the stellar population in a galaxy and can be used to estimate the SFR per unit stellar mass, SFR/M^* , (Brinchmann et al. 2004). The majority of star formation takes place preferentially in galaxies with low $D_n(4000)$ values. Considering all these restrictions, we have 1187 AGN and 1062 galaxies for the red subsamples and 1193 AGN and 1152 galaxies for the blue subsample (see Fig. 1 to test the environmental dependence on the distribution of properties).

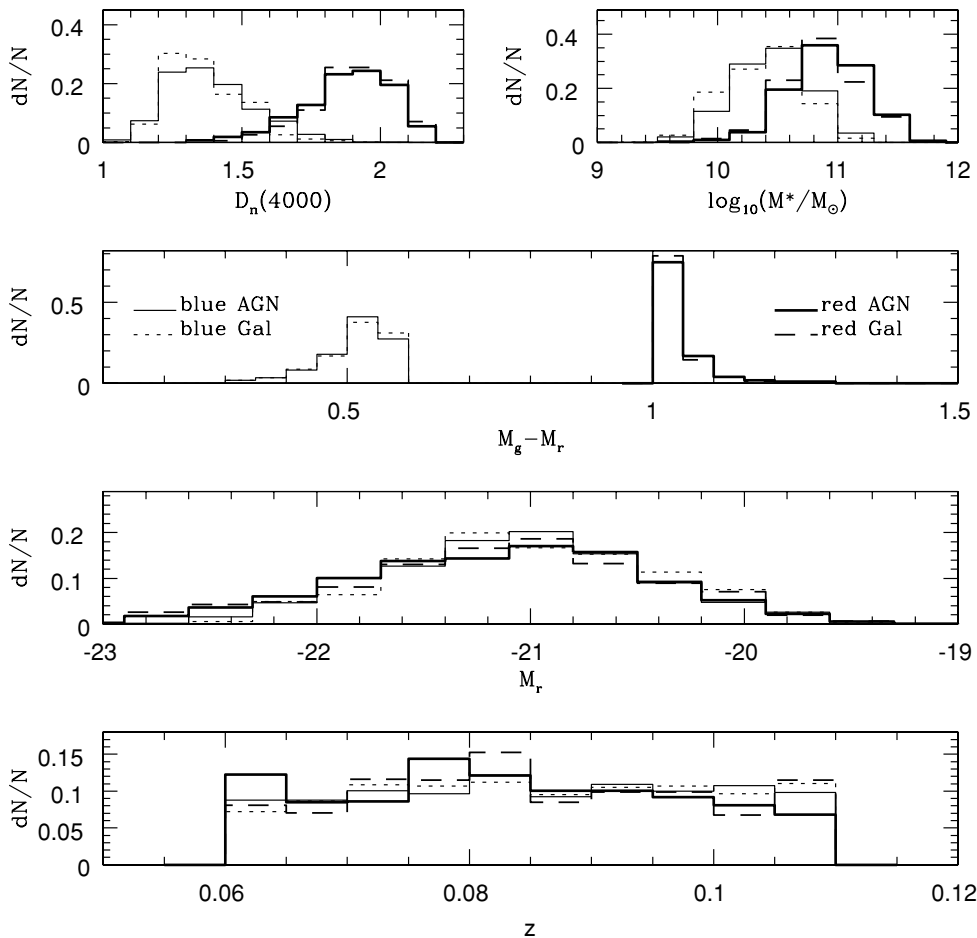


Figure 1. Normalized distributions of matched system properties: red AGN (thick solid line) and galaxies (dashed line) and blue AGN (thin solid line) and galaxies (dotted line).

3 CROSS-CORRELATION ANALYSIS

Several studies indicate that on average AGN and quasars populate regions with density enhancement similar to those of typical galaxies (Coldwell & Lambas 2006). The projected cross-correlation function calculated for a sample of AGN with a control sample of similar characteristics by Li et al. (2006) has revealed that AGN and galaxies inhabit dark matter haloes of similar mass. In this section, we explore the clustering properties between galaxies and blue and red AGN hosts and compare these results with control samples.

The large-scale clustering of galaxies is very well characterized by the two-point cross-correlation function, ξ . We have calculated the real-space, $\xi(r)$, cross-correlation function straightforward using the two-dimensional standard estimator $\Xi(\sigma, \pi)$ (Davis & Peebles 1983), where σ is the perpendicular distance and π is the distance parallel to the line of sight.

$$\xi(\sigma, \pi) = \frac{D_i D_j(\sigma, \pi) N_{R_i} N_{R_j}}{R_i R_j(\sigma, \pi) N_{D_i} N_{D_j}} - 1, \quad (2)$$

where $D_i D_j$ and $R_i R_j$ are the measured number of data–data and random–random pair counts respectively, binned as a function of the separation of the two variables σ and π , and N_{D_i} and N_{R_i} are the mean number densities of galaxies in the data and random samples. The random samples are created to have 10 times more objects, set to have the same radial and angular selection function as do the real catalogues. Integrating along the line of sight, where $\pi_{\max} = 60 h^{-1}$ Mpc,

$$\Xi(\sigma) = 2 \int_0^{\pi_{\max}} \xi(\sigma, \pi) d\pi, \quad (3)$$

we can estimate $\xi(r)$ by directly inverting $\Xi(\sigma)$ assuming a step function $\Xi(\sigma) = \Xi_i$ in bins centred in σ_i and interpolating between values for $r = \sigma_i$ Saunders, Rowan-Robinson & Lawrence (1992).

$$\xi(\sigma_i) = -\frac{1}{\pi} \sum_{j \geq i} \frac{\Xi_{j+1} - \Xi_j}{\sigma_{j+1} - \sigma_j} \ln \left(\frac{\sigma_{j+1} + \sqrt{\sigma_{j+1}^2 - \sigma_i^2}}{\sigma_j + \sqrt{\sigma_j^2 - \sigma_i^2}} \right) \quad (4)$$

The results are shown in Fig. 2. The error bars were calculated with the jackknife technique (Lupton 1993) by dividing the sample into 10 sky regions of approximately similar area. It is not unexpected that the red samples show stronger clustering than do the blue samples. The red early type galaxies are known to occupy regions of higher densities such as clusters or galaxy groups whereas the blue galaxies tend to be isolated or in the outer regions of such systems. A clear difference can be noticed between the red populations of active and non-active galaxies: red AGN are found in environments with lower densities at all scales than are their non-active counterparts. Such effect cannot be observed for the blue AGN sample which shows almost identical degree of large-scale clustering as the galaxy comparison sample. To further test the origin of the difference between active and non-active red galaxies, in the following section the density of AGN around groupings of galaxies is analysed.

Moreover, it is possible to observe that $\xi(r)$ shows two regimes with a transition from the linear to the non-linear case. The shape of $\xi(r)$ and specifically this transition could be related to the nature of the Halo model (Cooray & Sheth 2002) whereby in the inner regions of the correlation function galaxies belong to a same halo while for the outer regions the galaxies may populate different haloes. The transition between both regimes appears to be sensitive on the colour and luminosity of the galaxies. For the blue systems, the transition is seen to occur at smaller scales than for red ones,

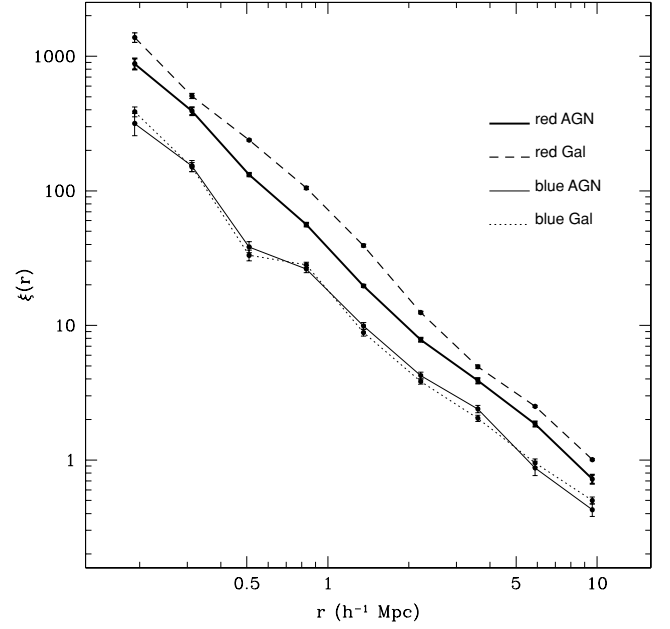


Figure 2. Real-space cross-correlation functions: red AGN (thick solid line) and galaxies (dashed line) and blue AGN (thin solid line) and galaxies (dotted line).

because red galaxies are generally found within galaxy systems, while blue galaxies are more often found in isolation.

4 DENSITY OF AGN AROUND GALAXY GROUPINGS

To determine the density of AGN within high-density environs, we use galaxy groups taken from Berlind et al. (2006). These galaxy groups were identified from the SDSS using an optimized redshift-space friends-of-friends (FOF) algorithm. The FOF linking lengths were selected to group together galaxies that occupy the same dark matter haloes (for details see Berlind et al. 2006).

In this section, we calculate the normalized mean density profile of AGN and non-active galaxies within a projected distance, $d_{\text{GCC}} < 3h^{-1}$ Mpc and with radial velocity differences, $\Delta V < 2000 \text{ km s}^{-1}$ with respect to the galaxy group centres. We conducted tests dividing the galaxy groups according to their richness expressed as the number of member galaxies. Fig. 3 shows the mean density profiles around galaxy groups with more than 15 members. The expected high density of red galaxies around group centres is noticeable, while for red AGN it is approximately four times lower within $250 h^{-1}$ kpc. The excess of red galaxies relative to red AGN around galaxy groups extends up to $\sim 1 h^{-1}$ Mpc. The mean density of the blue AGN on the other hand is considerably lower, and only a small difference between blue galaxies and blue AGN can be observed.

This result indicates that even though red AGN are associated with much richer environments than are blue AGN both samples are distributed differently compared to non-active red galaxies. That is to say, even when morphological segregation (Dressler 1980) is taken into account, red AGN are still preferentially located away from the centres of galaxy groups, a tendency that increases with group richness. More evidence of the nature of this effect is presented in the next section where we analyse the distribution of the morphological types of our galaxies.

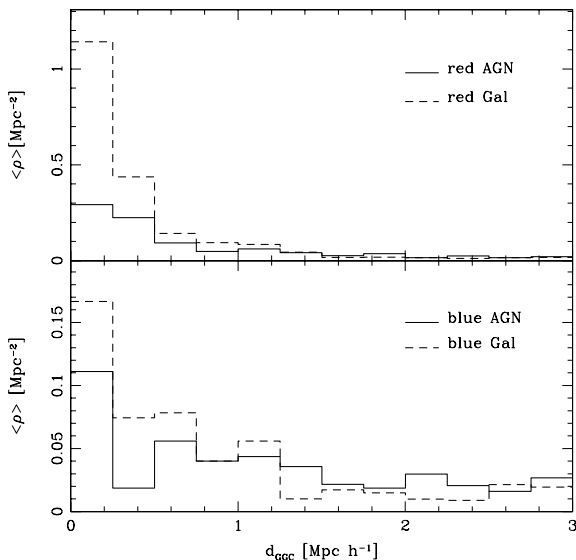


Figure 3. Mean density of galaxies (dashed lines) and AGN (solid lines) around Berlind’s galaxy groups with more than 15 members. The red samples are in the upper panel and the blue ones in the bottom panel.

Additionally, it is important to emphasize that the fraction of AGN decreases with number of galaxy group members and this effect is more evident for the red AGN. To illustrate this behaviour, we select all the galaxies and AGN within a group centre projected distance $d_{\text{GCC}} < 0.75 h^{-1} \text{ Mpc}$ and $\Delta V < 2000 \text{ km s}^{-1}$ where the lack of AGN is more pronounced as can be seen in Fig. 3. We show the relative distribution of AGN and galaxies as a function of richness, given by the number of galaxy group member, in Fig. 4 for red samples (top panel) and blue samples (middle panel). The diminishing number of AGN for galaxy systems with more than 10 members is perceptible for red AGN while for blue AGN this effect does not seem to be obvious.

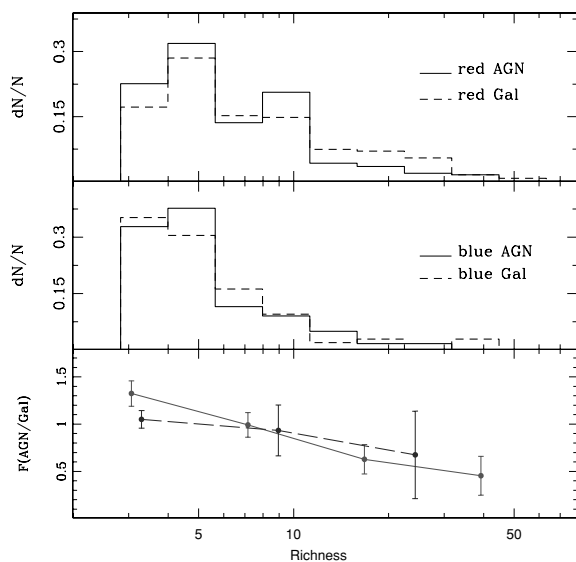


Figure 4. Relative distribution of AGN (solid lines) and galaxies (dashed lines) as a function of richness (in logarithmic scale), within $d_{\text{GCC}} < 0.75 h^{-1} \text{ Mpc}$ and $\Delta V < 2000 \text{ km s}^{-1}$ from the galaxy group centre. The red samples are in the upper panel and the blue ones in the middle panel. Bottom panel: fraction of AGN with respect to the galaxies, $F(\text{AGN}/\text{Gal})$, for red (solid line) and blue (long-dashed line) samples, respectively.

In order to quantify the dependence of the AGN presence with the richness of galaxy groups, we calculate the fraction of AGN with respect to the galaxies, $F(\text{AGN}/\text{Gal})$, for red and blue samples, respectively, as it is shown in Fig. 4 (bottom panel). It is possible to observe a clear deficiency of red AGN in the richest galaxy groups with respect to the red non-active galaxies. There is a strong relation between red AGN occurrence and the number of galaxy group members, while for blue AGN the relation is weak. Moreover, the evidence that the fraction of blue AGN remains almost constant with the richness is a signal that dominates the errors induced by the smaller number of blue AGN and galaxies in our rich galaxy groups.

Our results for red AGN are consistent with those of Popesso & Biviano (2006). They found an anticorrelation between the total fraction of AGN, with respect to the cluster members, and the velocity dispersion for two cluster samples. Their conclusion suggests that the increasing fraction of AGN versus the decreasing velocity dispersion is related to the merger rate since the merger rate has an inverse-cubic dependence on the velocity dispersion of the cluster or group, so it could explain the lack of the AGN fraction in richer systems.

5 MORPHOLOGIES OF AGN HOSTS

In contrast to bright type I AGN, the morphologies of the host galaxies of type II AGN are usually easily observable. The morphologies can be quantified using Sérsic profile (Sérsic 1963) that describes how the luminosity of a galaxy varies with distance from its centre, a generalization of the de Vaucouleurs and Freeman laws.

The Sérsic profile has the form

$$\ln I(R) = \ln I_0 - kR^{1/n}, \quad (5)$$

where I_0 is the intensity at $R = 0$. The parameter n , called the Sérsic index, controls the degree of curvature of the profile. The best-fitting value of n correlates with galaxy size and luminosity, such that bigger and brighter galaxies tend to be fit with larger values of n (Caon, Capaccioli & D’Onofrio 1993; Young & Currie 1994). Most galaxies are fit by Sérsic profiles with indices in the range $0.5 < n < 10$. Setting $n = 4$ gives the de Vaucouleurs profile which is a good description of giant elliptical galaxies. Setting $n = 1$ gives the Freeman exponential profile which is a good description of the light distribution of both disc galaxies and dwarf elliptical galaxies.

Fig. 5 illustrates the distribution of the Sérsic indices for red and blue AGN hosts relative to their non-active comparison samples. It is clear that red AGN have essentially the same morphological make-up as do the red non-active sample providing the final linchpin that the relative absence of AGN in cores of clusters and groups *cannot be explained simply as a consequence of morphological segregation*. Somewhat surprisingly, the morphologies of blue AGN are considerably different from the blue non-active galaxies despite their environs being almost identical at least in terms of their density. This finding leads to the question of whether or not the properties of the galaxies in these neighbourhoods are also different, a question we address in the following section.

However, we note from the distribution of the Sérsic indices of both samples that it is apparent that nuclear activity is a rare event in spiral discs and dwarf ellipticals. On the other hand, extended blue ellipticals seem to promote nuclear activity. Blue early-type galaxies have been shown to inhabit low-density environments away from cluster centres (Bamford et al. 2009) just like blue spirals,

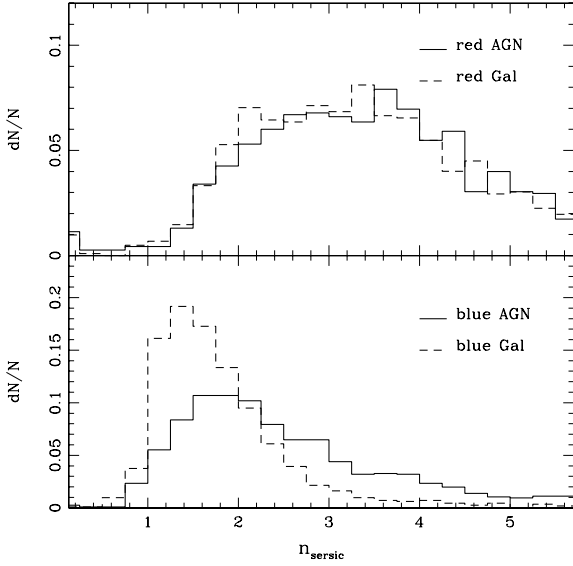


Figure 5. The distribution of the Sérsic index for red (top panel) and blue (bottom panel) samples for galaxies (dashed) and AGN (solid) lines. The Sérsic index provides a measure of the morphological type of a galaxy with lower numbers corresponding to spirals and higher numbers corresponding to ellipticals.

suggesting that the morphology of the host does play a role in triggering or sustaining nuclear activity.

6 PROPERTIES OF THE GALAXY NEIGHBOURHOODS

6.1 Dependence on host properties

The method commonly adopted for deriving a galaxy’s SFR is based on the modelled contribution of both the nebular emission by H II regions and diffuse ionized gas that are often combined and described in terms of an effective metallicity, ionization parameter, dust attenuation parameter at 5500 Å and dust to metal quotient (Bruzual & Charlot 1993; Charlot et al. 2002). Taking into account these factors, (Brinchmann et al. 2004) provide accurate estimates of total SFRs that are free from aperture bias.

Considering the results of the previous sections, one might expect that similar trends will be reflected in the properties of the neighbouring galaxies. Following the analysis of Coldwell & Lambas (2006), we analyse the colours $M_u - M_r$ and the logarithmic specific SFR $\log_{10}(\text{SFR}/M^*)$ ($\log_{10} \text{ yr}^{-1}$), where M^* is the estimated stellar mass, for galaxies surrounding the different targets.

In order to quantify any excess of blue (star-forming) galaxies in the AGN environs, we calculate the fraction of galaxies bluer than $M_u - M_r < 2.3$ approximately corresponding to the mean $M_u - M_r$ for the spectroscopic survey at $z < 0.1$ as well as the fraction of star-forming galaxies given by $\log_{10}(\text{SFR}/M^*) > -10.0$, both shown in Fig. 6. Tracer galaxies are selected to have projected distances $r_p < 3 h^{-1} \text{ Mpc}$ and radial velocity differences $\Delta V < 1000 \text{ km s}^{-1}$, relative to the target system.

Fig. 6 shows that the environs of both active and non-active blue systems are practically indistinguishable, whereas for the red systems significant differences are apparent. The environs of red AGN are populated by bluer galaxies with stronger star formation compared to the red non-active galaxies. The difference is approximately 3σ within $r_p < 1 h^{-1} \text{ Mpc}$, and this signal remains strong

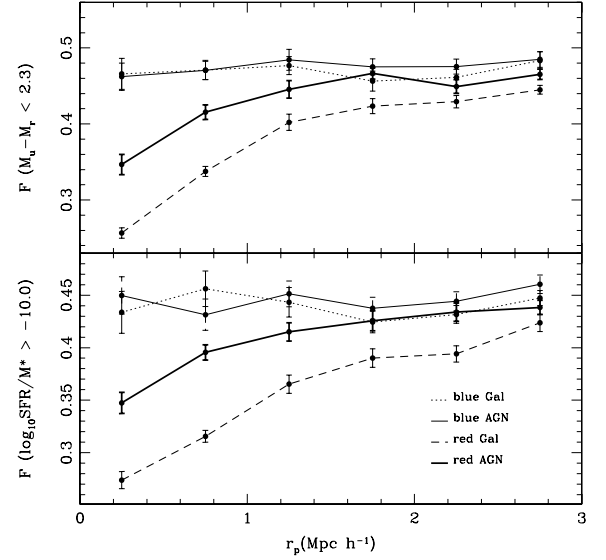


Figure 6. Fraction of $M_u - M_r$ blue (top panel) and star-forming (bottom panel) systems versus r_p : red AGN (thick solid line) and galaxies (dashed line) and blue AGN (thin solid line) and galaxies (dotted line).

beyond $r_p = 2 h^{-1} \text{ Mpc}$. This result is consistent with Coldwell & Lambas (2006) who find a higher fraction of blue star-forming galaxies associated with AGN environs without such a host colour discrimination. We observe no similarity in the excess of star-forming galaxies around the sample of red AGN compared to the non-active red galaxies (see Fig. 7).

We also calculate the fraction of blue and star-forming galaxies as a function of the luminosity, M_r , of the targets within $r_p < 2 h^{-1} \text{ Mpc}$ and $\Delta V < 1000 \text{ km s}^{-1}$ from the targets. We observe an excess of star-forming galaxies around red AGN compared with their non-active counterparts while the environment of blue systems remain clearly similar. We also notice a weak relation between the target luminosity and the calculated fraction. In general, low-luminosity AGN and non-active galaxies tend to populate regions where larger numbers of blue star-forming galaxies are also present.

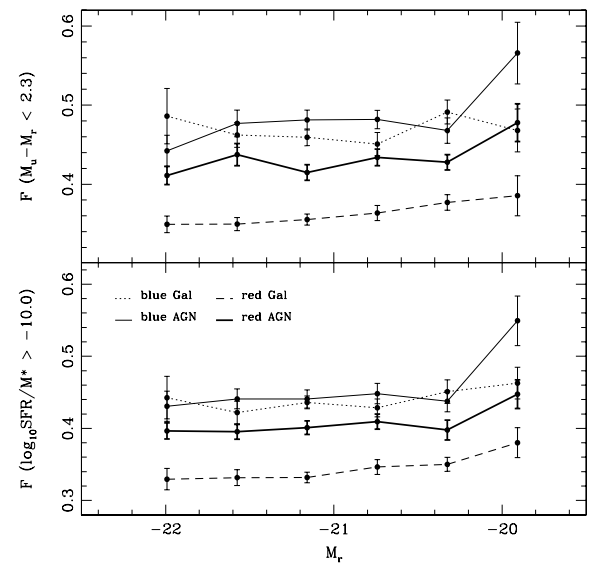


Figure 7. Fraction of blue (top panel) and star-forming (bottom panel) systems versus M_r : red AGN (thick solid line) and galaxies (dashed line) and blue AGN (thin solid line) and galaxies (dotted line).

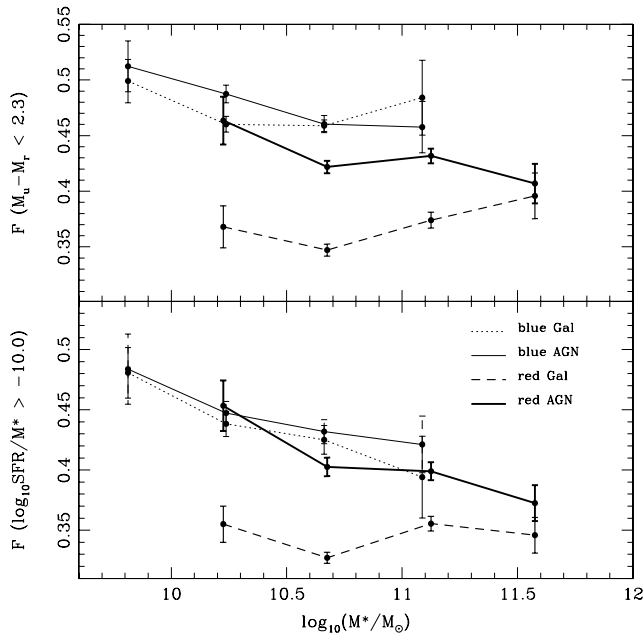


Figure 8. Fraction of blue and star-forming systems as a function of the stellar mass: red AGN (thick solid line) and galaxies (dashed line) and blue AGN (thin solid line) and galaxies (dotted line).

Moreover, the mass–luminosity relation in galaxies is well known. However, this relation has a significant spread that depends on the method used to derive the two parameters. Taking into account this caveat, at our level of completeness, we calculated the fraction of blue and star-forming galaxies as a function of the stellar mass, $\log_{10}(M^*/M_{\odot})$, of the targets, within $r_p < 2 h^{-1} \text{ Mpc}$ and $\Delta V < 1000 \text{ km s}^{-1}$. The results appear in Fig. 8 where a significant difference is observed between the environments of the red systems as function of their host stellar mass. This difference is larger for the less massive red AGN which show environmental properties not too dissimilar to those of more massive blue systems. One can see from Fig. 8 that the fraction of galaxies with $M_u - M_r < 2.3$ and $\log_{10}(\text{SFR}/M^*) > -10.0$ around blue systems and red AGN

decrease with M^* . No such trend is visible for the non-active red galaxies.

In addition, the values which characterize the neighbours of red AGN are much more comparable to those for the blue AGN and blue non-active galaxies. Even though they are not identical, the environments of the blue systems, AGN and non-active galaxies are practically indistinguishable within our errors.

6.2 Dependence on AGN activity

The relation between the AGN activity and host properties is a particularly interesting connection for study. To date, the most useful AGN activity parameter is the luminosity of the $[\text{O III}]\lambda 5007$ line ($L[\text{O III}]$), calculated by Kauffmann et al. (2003a). Although this line can be excited by massive stars as well as by AGN, it is known to be relatively weak in metal-rich, star-forming galaxies. The $[\text{O III}]$ line also has the advantage of being strong and easily detected in most galaxies, however, the narrow-line emission is likely to be affected by dust within the host galaxy (Kauffmann et al. 2003a), and thus it is important to correct for the effects of extinction. For AGN in SDSS, Kauffmann et al. (2003a) estimated the extinction using the Balmer decrement, finding that the best approximation for a dust correction to $L[\text{O III}]$ is based on the ratio $H\alpha/H\beta$.

By inspection of the relation between different parameters measured for the AGN hosts and the $L[\text{O III}]$ luminosities, we find a linear correlation between $D_n(4000)$ and $L[\text{O III}]$. Although we cannot rule out some contamination to the $L[\text{O III}]$ values from star-forming regions, this result indicates that AGN with higher values of $L[\text{O III}]$ most likely contain younger stellar populations than those with lower values of $L[\text{O III}]$ which are in a more evolved stage whereby gas deficiency causes a marked diminution in nuclear activity. Furthermore, a separation by galaxy colour implies a smooth separation by $L[\text{O III}]$ as it is shown in Fig. 9 (left-hand panel). Thus, a wide separation of two populations is visible, where the redder AGN hosts have very low values of $L[\text{O III}]$ compared with the bluer AGN.

Taking into account the correlation between the $M_g - M_r$ colours and $L[\text{O III}]$ showed in Fig. 9 (left-hand panel), we complete the analysis and select AGN samples with extreme values of $L[\text{O III}]$. We consider weak AGN to be those with $L[\text{O III}] < 6.45 L_{\odot}$ and powerful AGN to be those with $L[\text{O III}] > 7.07 L_{\odot}$ which are the

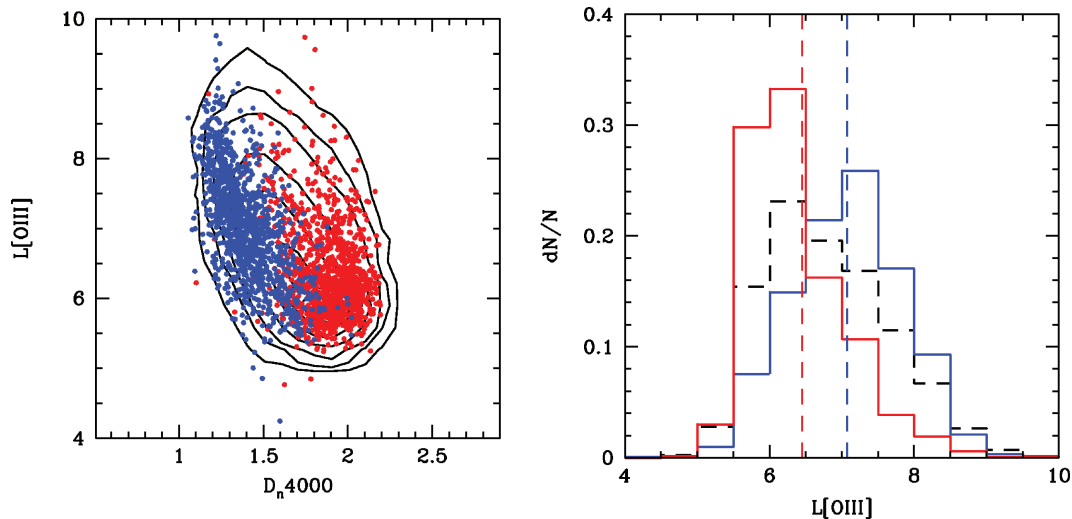


Figure 9. Left-hand panel: $L[\text{O III}]$ versus $D_n 4000$ for the total samples of AGN (contours), blue and red AGN (dots). Right-hand panel: $L[\text{O III}]$ distributions for the total sample of AGN (black dashed line), red AGN (solid red line) and blue AGN (solid blue line). The red and blue vertical dashed lines correspond to the mean values of $L[\text{O III}]$ of the red and blue AGN samples, respectively.

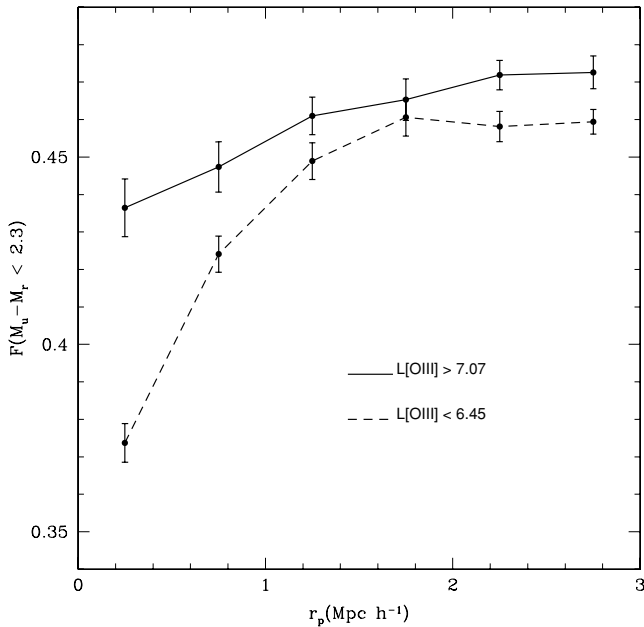


Figure 10. Blue galaxy fraction as a function of projected distance to weak (dashed line) and powerful (solid line) AGN. The values separating the powerful and weak AGN are taken from the mean values corresponding to the $L[O\text{III}]$ distribution of blue and red AGN, respectively (see Fig. 9).

mean of the $L[O\text{III}]$ values for the red and blue AGN samples, respectively (see Fig. 9, right-hand panel). Again, we calculate the fraction of blue galaxies within $r_p < 3 h^{-1} \text{ Mpc}$ and $\Delta V < 1000 \text{ km s}^{-1}$ of the host system. The results are shown in Fig. 10. As expected from the previous results, the powerful AGN are located in regions over populated by blue star-forming galaxies with respect to the weak AGN. Therefore, our results seem to indicate that the power of the AGN activity is strongly dependent on the environment of the host galaxies.

7 SUMMARY

In this paper, we investigate the environs that host type II AGN. In contrast with existing studies, we select two samples at the extremes of the colour distribution that we match to comparison samples of non-active galaxies. By focusing on the extreme colour ends of the AGN population, we are able to avoid averaging results across long baselines, and so too associated biases implicit in some of the earlier studies.

We find that the density distribution expressed by the cross-correlation function is almost identical for blue active and non-active host galaxies. In contrast, red active galaxies inhabit environments less dense compared to their red non-active counterparts. In spite of this, their environs are still considerably denser than those of blue hosts. In addition, two regimes are observed in the shape of the real-space cross-correlation function, $\xi(r)$, with a transition between its inner and outer regions related with the property that galaxies belong to only one or several haloes. This turning point seems to occur at smaller scales for blue systems, which are more often found in isolation, with respect to the red ones generally found within galaxy groups or clusters.

Moreover, the distribution of red AGN relative to galaxy groups and clusters shows a significant paucity or underpopulation at their centres. This cannot be explained by morphological segregation, since the morphological distributions of active and non-active red

systems are identical. Additionally, we note that the fraction of AGN decreases with number of galaxy group members and this effect is more evident for the red AGN. We find a strong relation between red AGN occurrence and the number of galaxy group members, while for blue AGN the relation is weak. This could suggest that the fraction of blue AGN remain almost constant with the richness taking into account the errors of the fraction due the small number of blue AGN and galaxy in rich galaxy groups.

On the other hand, the active and non-active blue systems have identical environments but markedly different morphological distributions. We note from the distribution of the Sérsic indices of the samples that it is apparent that nuclear activity is a rare event in spiral discs and dwarf ellipticals. The population of blue AGN hosts has a considerable contribution of ellipticals which are thought to be late-stage mergers with already-established morphology but remaining photometric anomalies (Marcum, Aars & Fanelli 2004). Blue early-type galaxies have been shown to inhabit low-density environments away from cluster centres (Bamford et al. 2009) just like blue spirals, suggesting that the morphology of the host does play a role in triggering or sustaining nuclear activity.

These results indicate that blue and red AGN might have intrinsically different formation mechanisms, suggestive of a dichotomy in the AGN population. Obviously, one could argue that such a dichotomy in the environment is a natural consequence of the sample selection derived from the antipoles of the AGN population. For example, according to a review by Storchi-Bergmann (2008), nuclear activity outlives star formation and in some cases its onset might be even delayed until after the star formation period is triggered in the same episode. In such a scenario, the blue AGN in our sample would mark mainly the onset of this activity and red AGN its final stage. In this sense, one could interpret our blue sample to indeed fulfil this general idea: (i) morphology plus colour combination suggesting recent galaxy interactions; (ii) high SFR; (iii) young stellar population; (iv) strong nuclear activity and (v) scaling of nuclear power with age of the stellar population indicating gradual depletion of fuel.

The $L[O\text{III}]$ versus $D_n(4000)$ distribution (nuclear power versus age of stellar population) of all AGN appear to naturally follow the trend set by our blue sample with exception of the extremely red AGN. The red AGN in our sample are much older than would otherwise be suggested by an extrapolation of the trend marked by the blue and intermediate-colour AGN. Thus, to belong to the same population as the blue AGN their stellar population would need to age at an accelerated rate. We revisited some possible scenarios.

In a first scenario, a blue galaxy with an AGN would enter a cluster, be stripped of its gas envelope, leading to starvation (Balogh, Navarro & Morris 2000), while the gas content at its centre is withheld at the deepest position in the galaxy potential well. Thus, the AGN could continue to be fed while the star formation is effectively halted throughout most of the galaxy. The problem is that the stripping of gas does not accelerate aging, but simply truncates the star formation. It means that galaxies would not show ongoing star formation but would still have relatively young populations considering the short duration of a typical burst of nuclear activity.

In the second scenario, the extremely red AGN have a separate trigger mechanism that occurs when an already-dormant AGN enters into the strong gravitational potential of a galaxy cluster. The potential is known to strip some of the entering galaxies of their gas, however, not all of them. The observations of brightest cluster galaxies have found recent star formation in one-third of those cluster core objects (Loubser et al. 2008) suggesting that not all of the cluster galaxies are stripped of their gas when passing through

the cluster potential. In this context, some galaxies will be stripped completely, some lose the gas in outer regions and some others may capture some of this deposited gas from the intracluster medium. Thus, an old, red, massive galaxy containing a dormant supermassive black hole might acquire new gas supplies from the intracluster medium. The gravitational potential of the cluster would assist in efficient transportation of the captured as well as galaxy's own gas component into the central black hole, triggering a burst of nuclear activity and resurrection of the AGN. In this scenario, the red AGN correspond to a recycled species.

ACKNOWLEDGMENTS

We thank the anonymous referee for helpful suggestions and comments. This research was partially supported by grants from CONICET, Agencia Córdoba Ciencia and the Secretaría de Ciencia y Técnica de la Universidad Nacional de Córdoba.

Funding for the SDSS and SDSS II has been provided by the Alfred P. Sloan Foundation, the Participating Institutions, the National Science Foundation, the U.S. Department of Energy, the National Aeronautics and Space Administration, the Japanese Monbukagakusho, the Max Planck Society and the Higher Education Funding Council for England. The SDSS website is <http://www.sdss.org/>.

The SDSS is managed by the Astrophysical Research Consortium for the participating institutions. The participating institutions are the American Museum of Natural History, Astrophysical Institute Potsdam, University of Basel, University of Cambridge, Case Western Reserve University, University of Chicago, Drexel University, Fermilab, the Institute for Advanced Study, the Japan Participation Group, Johns Hopkins University, the Joint Institute for Nuclear Astrophysics, the Kavli Institute for Particle Astrophysics and Cosmology, the Korean Scientist Group, the Chinese Academy of Sciences, Los Alamos National Laboratory, the Max-Planck-Institute for Astronomy, the Max-Planck-Institute for Astrophysics, New Mexico State University, Ohio State University, University of Pittsburgh, University of Portsmouth, Princeton University, the United States Naval Observatory, and the University of Washington.

REFERENCES

- Alonso M. S., Lambas D. G., Tissera P. B., Coldwell G., 2007, *MNRAS*, 375, 1017
- Baldwin J. A., Phillips M. M., Terlevich R., 1981, *PASP*, 93, 5
- Balogh M. L., Navarro J. F., Morris S. L., 2000, *ApJ*, 540, 113
- Bamford S. P. et al., 2009, *MNRAS*, 393, 1324
- Begelman M. C., Blandford R. D., Rees M. J., 1980, *Nat*, 287, 307
- Berlind A. A. et al., 2006, *ApJS*, 167, 1
- Biviano A. et al., 1997, *A&A*, 321, 84
- Blanton M. R. et al., 2003, *ApJ*, 594, 186
- Brinchmann J., Charlot S., White S. D. M., Tremonti C., Kauffmann G., Heckman T., Brinkmann J., 2004, *MNRAS*, 351, 1151
- Bruzual A. G., Charlot S., 1993, *ApJ*, 405, 538
- Caon N., Capaccioli M., D'Onofrio M., 1993, *MNRAS*, 265, 1013
- Charlot S., Kauffmann G., Longhetti M., Tresse L., White S. D. M., Maddox S. J., Fall S. M., 2002, *MNRAS*, 330, 876
- Coldwell G. V., Lambas D. G., 2003, *MNRAS*, 344, 156
- Coldwell G. V., Lambas D. G., 2006, *MNRAS*, 371, 786
- Cooray A., Sheth R., 2002, *Phys. Rep.*, 372, 1
- Davis M., Peebles P. J. E., 1983, *ApJ*, 267, 465
- Dressler A., 1980, *ApJ*, 236, 351
- Dressler A., Thompson I. B., Shectman S. A., 1985, *ApJ*, 288, 481
- Fukugita M., Ichikawa T., Gunn J. E., Doi M., Shimasaku K., Schneider D. P., 1996, *AJ*, 111, 1748
- Gaskell C. M., 1985, *Nat*, 315, 386
- Hernquist L., Mihos J. C., 1995, *ApJ*, 448, 41
- Kauffmann G., Haehnelt M. G., 2002, *MNRAS*, 332, 529
- Kauffmann G. et al., 2003a, *MNRAS*, 346, 1055
- Kauffmann G. et al., 2003b, *MNRAS*, 341, 33
- Kauffmann G., White S. D. M., Heckman T. M., Ménard B., Brinchmann J., Charlot S., Tremonti C., Brinkmann J., 2004, *MNRAS*, 353, 713
- Koulouridis E., Plionis M., Chavushyan V., Dultzin-Hacyan D., Krongold Y., Goudis C., 2006, *ApJ*, 639, 37
- Lake G., Katz N., Moore B., 1998, *ApJ*, 495, 152
- Li C., Kauffmann G., Wang L., White S., Heckman T., Jing Y., 2006, *MNRAS*, 373, 457
- Loubser S. I., Sansom A. E., Sánchez-Blázquez P., Söchtig I. K., Bromage G. E., 2008, *MNRAS*, 391, 1009
- Lynden-Bell D., 1969, *Nat*, 223, 690
- Lupton R. H., 1993, *Statistics in Theory and Practice*. Princeton Univ. Press, Princeton, NJ
- Marconi A., Hunt L., 2003, *ApJ*, 589, L21
- Marcum P. M., Aars C. E., Fanelli M. N., 2004, *AJ*, 127, 3213
- Miller C. J., Nichol R. C., Gómez P. L., Hopkins A. M., Bernardi M., 2003, *ApJ*, 597, 142
- Petrosian V., 1976, *ApJ*, 209, 1
- Popesso P., Biviano A., 2006, *A&A*, 460, L23
- Roos N., 1981, *A&A*, 104, 218
- Roos N., 1985, *A&A*, 294, 479
- Sanders D. B., Soifer B. T., Scoville N. Z., 1988, *Sci*, 239, 625
- Saunders W., Rowan-Robinson M., Lawrence A., 1992, *MNRAS*, 258, 134
- Serber W., Bahcall N., Menard B., Richards G., 2006, *ApJ*, 643, 68
- Sérsic J. L., 1963, *Bol. Asoc. Argentina. Astron.*, 6, 41
- Shlosman I., Begelman M. C., Frank J., 1990, *Nat*, 345, 679
- Smith R. J., Boyle B. J., Maddox S. J., 1995, *MNRAS*, 277, 270
- Söchtig I. K., Clowes R. G., Campusano L. E., 2002, *MNRAS*, 331, 569
- Söchtig I. K., Clowes R. G., Campusano L. E., 2004, *MNRAS*, 347, 1241
- Sorrentino G., Radovich M., Rifatto A., 2006, *A&A*, 451, 809
- Storchi-Bergmann T., 2008, *Rev. Mex. Astron. Astrofis. Ser. Conf.*, 32, 139
- Strauss M. et al., 2002, *AJ*, 124, 1810
- Toomre A., Toomre J., 1972, *ApJ*, 178, 623
- Tremaine S. et al., 2002, *ApJ*, 574, 740
- Tremonti C. et al., 2004, *ApJ*, 613, 898
- York D. G. et al., 2000, *AJ*, 120, 1579
- Young C. K., Currie M. J., 1994, *MNRAS*, 268, 11

This paper has been typeset from a $\text{\TeX}/\text{\LaTeX}$ file prepared by the author.